Bioinspired Lotus Fiber-Based Graphene Electronic Textile For Gas Sensing

Da Yeon Cheong
Korea University - Sejong Campus
Sang Won Lee
Korea University - Anam Campus: Korea University
Hyo Gi Jung
Korea University - Anam Campus: Korea University
Seokbeom Roh
Korea University - Sejong Campus
Dongtak Lee
Korea University - Anam Campus: Korea University
Taeha Lee
Korea University - Sejong Campus
Saebomeena Lee
Korea University - Sejong Campus
Wonseok Lee
Korea National University of Transportation
Dae Sung Yoon
Korea University - Anam Campus: Korea University
Gyudo Lee (lkd0807@korea.ac.kr)
Korea University - Sejong Campus https://orcid.org/0000-0001-7895-5112

Research Article

Keywords: Lotus fiber, Cellulose fiber, Graphene, Wearable device, Electronic textile, Nitrogen dioxide

Posted Date: November 16th, 2021

DOI: https://doi.org/10.21203/rs.3.rs-1001747/v1

Version of Record: A version of this preprint was published at Cellulose on March 31st, 2022. See the published version at https://doi.org/10.1007/s10570-022-04541-6.

Abstract

Graphene electronic textiles (e-textiles) have attracted significant attention in various sensing applications owing to their strong advantages. During the fabrication of these textiles, there are factors to consider, such as electrical conductivity, mechanical flexibility, weight, and applicability in other practical applications. Bioinspired lotus fiber has appropriate advantages to be used as graphene e-textiles, including lightweight (<1 mg), eco-friendliness, crease-resistant, pilling resistance, and flexibility. However, lotus fiber-based graphene e-textiles have not yet been reported. In this study, we developed a reduced graphene oxide–coated lotus fiber (RGOLF) which was successfully fabricated by the hydrogen interaction between graphene flakes and cellulose fiber. The RGOLF exhibited a higher electrical conductivity (4.63 ± 0.22 μS) and a remarkable sensing performance for hazardous NO_2 gas molecules within a short exposure time (~3 min), including a low detection limit (~1 ppm), selectivity, and resistance to relative humidity. Moreover, we verified the mechanical flexibility of RGOLF through a 1,000-cycle bending test. These results suggest that the bioinspired RGOLF could be used as a gas sensor in environmental air with a strong potential for use in various wearable applications.

1. Introduction

Electronic textiles (e-textiles) have attracted significant attention in various applications, including chemical gas sensors (Lee et al. 2020; Lee et al. 2021a; Lee et al. 2021b), energy harvesting (Abdelkader et al. 2017; Liu et al. 2015a), and electrochemical sensors for bio-signal detection (Kinnamon et al. 2018; Hu et al. 2020). E-textiles have many advantages, such as portability, flexibility, high conductivity, and lightweight, making them suitable for application as wearable devices (Stoppa and Chiolerio 2014; Kan and Lam 2021; Lee et al. 2021a). Specifically, graphene e-textiles have been widely developed in sensing technologies, such as electrochemical biosensors (Coyle et al. 2007), pressure sensors (Li et al. 2019), motion sensors (Wang et al. 2020), and electronic skin (Chun et al. 2019). Moreover, graphene e-textiles have been advanced as chemical gas sensors for detecting hazardous gases, such as nitrogen dioxide (NO_2) (Lee et al. 2021b), ammonia (NH_3) (Lee et al. 2020), carbon monoxide (CO) (Utari et al. 2020), and hydrogen (Zhu et al. 2021).

To fabricate the graphene e-textiles, graphene has been attempted to coat on various 1-dimensional textiles (e.g., cotton yarn, nylon-6 yarn, and polyester yarn) (Lee et al. 2021b; Lee et al. 2020; Yun et al. 2013; Ju Yun et al. 2015). According to the literature, graphene e-textiles exhibit mechanical flexibility, washability, and the ability to sense toxic gases (Lee et al. 2020; Lee et al. 2021b). Thus, graphene e-textiles have the potential to be used as wearable sensors for detecting toxic gases and even for monitoring human health from their breath. However, to improve electrical conductivity, which is an essential component of wearable sensors, textiles are required to be functionalized with adhesive molecules for attaching abundant graphene flakes. Textile surfaces have been functionalized using various biomolecules (e.g., bovine serum albumin, dopamine, globular/fibrous protein) (Ju Yun et al. 2015; Lee et al. 2020; Lee et al. 2021b), and organic molecules (Kang et al. 2018), resulting in highly conductive graphene e-textiles. Metal/metallic nanoparticles (e.g., Au, and Ni) have also been composed

in the fabrication of highly conductive graphene e-textiles (Yun et al. 2017; Liu et al. 2015b). However, to obtain highly conductive e-textiles, previous 1-dimensional textile requires a gluing of their surface with adhesive molecules or fabrication of the graphene composites with nanoparticles. Moreover, the yarn-based graphene e-textiles are not suitable for use as wearable sensors because of their weight (~22 mg) (Lee et al. 2021a).

To address these issues, graphene e-textiles were fabricated on 2-dimensional textiles (e.g., polyester sheet, and nylon-6 mesh fabric) (Lee et al. 2021a; Park et al. 2018). These graphene e-textiles showed remarkable performance for sensing gas molecules, mechanical flexibility, and washability. Moreover, it has approximately 19 times lighter than the yarn-based graphene e-textiles (Lee et al. 2021a). However, they still require the adhesive glues to improve electrical conductivity that would enable the attainment of good sensing efficiency for toxic gases. Further, it is difficult to employ 2-dimensional textiles in various applications owing to their lattice structure. Therefore, we endeavored to identify a 1-dimensional textile that is appropriate for use as a wearable device and widely expandable for applications.

Lotus fiber (*Nelumbo nucifera*), an aquatic cellulosic fiber, could be a promising candidate as a template for e-textiles owing to its lightweight (<1 mg), eco-friendly, crease-resistant, pilling resistant, and flexible properties (Sangita Tomar 2019). Furthermore, the functional groups on cellulose fiber could bind with graphene flakes via hydrogen interaction, which allows for its improvement of the electrical conductivity with no use of adhesive materials. In this regard, we developed a reduced graphene oxide-coated lotus fiber (RGOLF). The physical and chemical properties of the RGOLF were analyzed microscopically and spectroscopically. We characterized the electrical properties according to the RGOLF thickness. Finally, the RGOLFs were attempted to detect toxic NO_2 gas molecules. The RGOLF exhibited good enough sensing performance, including a low detection limit, selectivity, and resistance to relative humidity. Furthermore, we confirmed that the RGOLF could be a wearable gas sensor, through mechanical flexibility up to 1,000 times of bending test. Taken together, these results suggest that the RGOLF could form the next generation of 1D graphene e-textiles for various applications.

2. Materials And Methods

2.1. Materials

Graphene oxide (GO) solution was purchased from Graphene Supermarket, Inc. (USA). The optimal concentration of the GO solution was adjusted using distilled water (DW, ThermoFisher, USA). For chemical reduction of GO, we purchased a hydriodic acid (57 wt% in H_2O), sodium bicarbonate (>99.7%), and acetic acid solution from Sigma Aldrich (USA).

2.2. Preparation of the lotus fibers

Lotus fiber (LF) was obtained from the stem of *Nelumbo nucifera* harvested from nature (Pandey et al. 2020). Before preparing LF, the stems were washed using DW and dried at room temperature (23°C). We obtained several strands of cellulose fibers by cutting the outer skin of the lotus peduncle and pulling it

on both sides. Bare LF was prepared into a single strand (length: ~20 cm) by twisting and gathering several strands of cellulose fibers (Fig. 1a-c). Bare LF was then dried in a fume hood.

2.3. Fabrication of RGOLF

Reduced graphene oxide-coated lotus fibers (RGOLFs) were fabricated using bare LF and GO solution (Fig. 1a-c). Through a dip-coating method, the bare LFs were soaked in a 3 g/L GO solution for 2 h to uniformly coat the GO flakes onto the LF surface, resulting in a GO-coated LF (GOLF) (Lee et al. 2021b). The GOLF was dried in a fume hood before the chemical reduction of the GO flakes. The GO flakes on the GOLF surface were transformed into reduced graphene oxide (RGO) flakes using the commonly used chemical reduction method (Lee et al. 2020; Lee et al. 2021b; Lee et al. 2021a). In detail, the GOLF was immersed in a vial containing 2 mL of hydriodic acid solution and 5 mL of acetic acid solution. The chemical reduction proceeded under 40°C for 2 h. Subsequently, the fibers were washed several times using saturated sodium bicarbonate solution and DW to remove the residual reducing agent. The brownish color of GOLF turned black after GO reduction (Fig. 1d) (Lee et al. 2020; Lee et al. 2021b). The RGO-coated LF (RGOLF) was dried under a fume hood maintained at room temperature.

2.4. Characterization

The morphology of GO flakes was characterized using field-emission transmission electron microscopy (FE-TEM, JEM-2100F, JEOL, Japan) and atomic force microscopy (AFM, Multimode 8, Bruker). AFM imaging was operated in the tapping mode under ambient air. The height of GO flakes was analyzed using Nanoscope Analysis software (Bruker). Furthermore, the morphology of the fibers was characterized using a scanning electron microscope (SEM, JEOL-7610F-Plus, JEOL, Japan). For high-resolution SEM imaging, a Pt layer (~12 nm thick) was coated on the fiber surface using a sputter coater (108 auto, Cressington Scientific Instruments Inc., UK) with a deposition rate of 0.83 Å/s for 150 s (Lee et al. 2020). SEM imaging was performed at a high voltage (10 kV). A microscopic image of bare LF was obtained using an optical microscope (DS-Ri2, Nikon, Japan) to measure the diameter.

Chemical characterization of the fibers (including the GOLF, and the RGOLF) was performed to compare the chemical differences before and after the GO reduction by using Raman spectroscopy and X-ray photoelectron spectroscopy (XPS) (Ferrari and Basko 2013; Lee et al. 2021a). The Raman spectra were obtained by Raman spectroscopy (LabRam Aramis, Horriba Jovin Yvon, USA) using a 563 nm excitation laser. The XPS (K-alpha, Thermo VG, UK) analysis was carried out with a sampling area (400 × 400 μm^2) in a vacuum (4.8×10^{-9} mbar), using a monochromatic Al X-ray source at 1486.6 eV.

The electrical conductivity of all fibers was characterized using a commercial current-voltage (I-V) meter (Cantis Inc., South Korea) (Lee et al. 2018b). Two probes from the I-V meter were connected to both ends of the fiber (3 cm in length) (Lee et al. 2020). Simultaneously, the electric current was recorded on a computer. The applied voltage (2 V) and sweep mode (from -2 to 2 V) were controlled using the enclosed software. We measured the initial electrical conductivity at 2 V before the exposure of RGOLF to NO_2. The experiment was performed at 23°C (room temperature) and 26% relative humidity.

2.5. Exposure of the RGOLF to gas molecules

The RGOLF was placed in a gas chamber for exposure to NO_2 (i.e., the target gas). The volume (500 sccm) and concentration (0 – 100 ppm) of the gas were regulated by using a home-built mass flow controller (MFC) (Lee et al. 2018b; Lee et al. 2021b). The NO_2 concentration was controlled by mixing it with an inert pure nitrogen gas (i.e., the base gas) in the MFC. To characterize gas detectability, the electric current of RGOLF was measured at an applied voltage of 2 V after gas exposure. The gas detectability test was conducted in a laboratory where the temperature was maintained at 21°C and 28% relative humidity.

2.6. Selectivity and relative humidity test of the RGOLF

The selectivity and humidity tests of the RGOLF were conducted *via* various gases and relative humidity (20 – 99%). Each RGOLF was exposed to various gases, including nitrogen (>99%, N_2), ethanol (10 ppm, C_2H_5OH), carbon monoxide (10 ppm, CO), acetone (100 ppm, C_3H_6O), ammonia (100 ppm, NH_3), and NO_2 (10 ppm). For the humidity test, relative humidity (20 – 99%) was controlled by changing the mixing ratio of fully humid air and dry air. Humidity was confirmed using a humidity sensor. The electric current of the RGOLFs was measured by using an I-V meter before and after exposure to various gases or relative humidity.

2.7. Bending test of the RGOLF

We carried out a bending test of the RGOLF (5 cm in length) using a computer-controlled actuating system (EA10.X/HD, Step Lap, Italy) (Lee et al. 2021b). One end of the RGOLF was held on a fixed stage, and the other end was held on a movable stage. The elongation and compression of the RGOLF proceeded in one cycle. The bending test was repeated for up to 1,000 cycles at a scan rate of 1 cm/s. The electric current of RGOLF was measured after every 50 cycles of bending. The test was performed in a laboratory where the temperature was maintained at 20°C and 25% relative humidity.

3. Results And Discussion

The schematic illustration shows the fabrication steps for a reduced graphene oxide-coated lotus fiber (i.e., RGOLF) (Fig. 1a). We prepared lotus fiber (LF) from *Nelumbo nucifera* with various diameters (150 – 300 μm) for use as an e-textile platform (Fig. 1b) (Wu et al. 2014). As well known, microscopic analyses have demonstrated that the LFs have pilling resistance (Fig. 1c) (Sangita Tomar 2019). The detailed information is provided in the Experimental Section. Graphene oxide-coated lotus fiber (GOLF) was fabricated by coating bare LF with GO flakes (3 g/L) through a dip-coating method (Ju Yun et al. 2015). Through chemical reduction, brownish-colored GOLF was converted to black-colored fiber (Fig. 1d) (Lee et al. 2020; Ju Yun et al. 2015). This indicated that the GO flakes were well transformed into reduced graphene oxide (RGO) flakes, resulting in RGOLF (Lee et al. 2021b; Lee et al. 2021a). At applied voltages ranging from -2 to 2 V, the RGOLF exhibited high electrical conductivity, whereas both bare LF and GOLF

exhibited insulating properties (Fig. 1e). It also implied that the RGO flakes were well transformed and stably attached to the LF surface.

Chemical analysis of the fibers (GOLF, and RGOLF) was performed to confirm whether RGO flakes were reduced from GO flakes (height, ~1 nm) (Fig. 2a and b) (Lee et al. 2020). From the Raman spectrum, both fibers exhibited intrinsic graphene peaks, including the *D* and *G* peaks at 1342.34 cm^{-1}, and 1595.89 cm^{-1}, respectively (Ferrari and Basko 2013). This means that the graphene flakes (GO, and RGO) were well attached to the LF surface (Fig. 2c) (Lee et al. 2021b; Lee et al. 2021a; Lee et al. 2020). After GO reduction, the I_D/I_G ratio increased from 0.91 to 1.19, which is attributed to the decrease in the *G* peak intensity (Lee et al. 2020; Moon et al. 2010). In XPS analysis, the GOLF and RGOLF depicted both C 1s and O 1s peaks, which were derived from graphene derivatives (Fig. 2d) (Ju Yun et al. 2015; Lee et al. 2021b). The intensity of the O 1s peak at 532.24 eV was diminished by 61.55% after GO reduction, indicating the chemical reduction of GO flakes (Lee et al. 2021a). Furthermore, the intensity of the C–O peak in the XPS C 1s spectra decreased from 34.96–33.95% after GO reduction, signifying that the RGO flakes on RGOLF were successfully transformed from the GO flakes on GOLF (Figure S1 and Table S1in Supplementary Information) (Lee et al. 2018b). The N 1s peak was observed in both GOLF and RGOLF, which is derived from amino acids in the LF (Pandey et al. 2020; Johansson et al. 2020). Both chemical analysis results revealed that the GO flakes were well bound on the LF without any additional adhesive materials, and the RGO flakes on RGOLFs were well transformed from GO flakes on the GOLFs through chemical reduction. Interestingly, without adhesive materials, the RGOLFs (9.31 ± 0.40 μA at 2 V of applied voltage) exhibited higher electrical conductivity, compared to the conventional cotton yarn-based graphene e-textiles (3.42 ± 0.01 μA at the 2 V), as shown in our previous work (Lee et al. 2021b). This might be attributed to the hydrogen interactions between GO flakes and cellulose (i.e., LF) (Chen et al. 2018; Xu et al. 2015). Therefore, compared to the conventional cotton yarn-based graphene e-textiles, we successfully developed graphene e-textiles (RGOLF) with high electrical conductivity without any side-effects from the insulating adhesive proteins (i.e., globular proteins, and amyloid nanofibrils) (Lee et al. 2021b).

The morphological characteristics of the fibers (LF, GOLF, and RGOLF) were obtained by using SEM (Fig. 3). We observed a distinct difference between the fibers before and after the GO coating. The bare LF has no distinctive features on its surface, whereas both fibers (GOLF and RGOLF) exhibited numerous wrinkles and ripples on their surface after GO attachment (Lee et al. 2021b; Ju Yun et al. 2015). The images showed that the GO flakes were well attached to the surface of the GOLF, as well as the RGOLF. Additionally, the SEM images confirmed that the RGOLFs were appropriately fabricated using LF and graphene.

Before exposure to NO_2, we prepared the RGOLFs with various GO concentrations (1 – 3 g/L) to analyze their electrical characteristics (Fig. 4). The results indicated that the electric current of RGOLF increased as the GO concentration increased (Fig. 4a). Specifically, an electric current of RGOLF fabricated using 3 g/L of GO was measured to be 22.87 μA at 2 V. Meanwhile, both bare LF and GOLF exhibited an insulating property at the applied voltage range (from -2 to 2 V). The electrical characteristics of RGOLFs

were empirically investigated using RGOLFs fabricated with GO flakes (3 g/L) and various diameters (150 – 300 μm) of LF (Fig. 4b). It showed that the greater the diameter of LF, the greater the electric current was measured; 1.76 ± 0.10 μA in RGOLF with 150 μm, 3.05 ± 0.32 μA in RGOLF with 200 μm, 4.70 ± 0.24 μA in RGOLF with 250 μm, and 9.31 ± 0.40 μA in RGOLF with 300 μm) (Table S2). Similarly, electrical conductance increased as the LF diameter increased. At the same applied voltage (2 V), the RGOLF fabricated with 3 g/L GO and 300 μm diameter showed the highest conductance (4.63 ± 0.22 μS) (Table S2). The electrical conductance (G) was obtained using the following equation, where ΔV is the increment of the applied voltage (0.1 V), and ΔI is the change in the measured current when ΔV occurs.

$$G = \frac{\mathrm{I}_1 - \mathrm{I}_2}{\Delta \mathrm{V}} = \frac{\Delta \mathrm{I}}{\Delta \mathrm{V}}, \mathrm{V} = -2\mathrm{to}2\mathrm{V} (1)$$

For practical application, we exposed NO_2 to RGOLFs fabricated with the optimized concentration of GO (3 g/L) on LF (diameter: 300 μm). NO_2 gas detectability was scrutinized using the RGOLF (Fig. 5a). The RGOLFs were exposed to various NO_2 concentrations (1 – 10 ppm), and their response characteristics were measured (Fig. 5b). Noted that NO_2 gas has harmful effects not only environmental pollution, such as mild dust, acid rain, and destruction of the ozone layer, but also on human health, causing nausea, throat/eye irritation, and respiratory disease. According to the literature (Lee et al. 2018a; Lee et al. 2021b), the specific concentration (10 ppm) of NO_2 is known to be the threshold concentration that induces a fatal effect on human health. Long-term exposure to 10 ppm NO_2 causes nose/throat discomfort, transient cough, eye irritation, fatigue, and nausea (Ou et al. 2015; Elsayed 1994).
In this regard, we exposed the RGOLF to various concentrations (1 – 10 ppm) of NO_2s for 3 min. As shown in Fig. 5b, the electric current increased with increasing NO_2 concentration, exhibiting linearity (R^2 = 0.997). The changes in electric current ($\Delta I = I - I_0$) were measured at the applied voltage of 2 V. I_0 and I denote the electric current before and after exposure to gas, respectively. In detail, the electric current was increased to 0.24 ± 0.02 μA, 0.44 ± 0.04 μA, 0.63 ± 0.03 μA, 0.81 ± 0.11 μA, 1.10 ± 0.05 μA, and 1.34 ± 0.14 μA with 1, 3, 5, 7, 9, and 10 ppm NO_2, respectively.

The selectivity and relative humidity resistance were investigated by exposing RGOLFs to various gases or relative humidity (20 – 99%). In terms of the selectivity test, RGOLF responded well to NO_2 (10 ppm) but barely responded to other gases such as N_2 (99%), C_2H_5OH (100 ppm), CO (10 ppm), C_3H_6O (100 ppm), and NH_3 (100 ppm) (Fig. 5c). The electrical response was defined using the following equation:

Response = $(I - I_0)/ I_0 \times 100(\%)$ (2)
There was a small negative response to NH_3 (100 ppm), which was attributed to the fact that NH_3 molecules act as electron donors on the RGO flakes, resulting in a small decrease in the electrical response (Leenaerts et al. 2008; Lee et al. 2020). From the electrical response to NH_3 exposure, it seems that the RGOLF could be used for detecting NH_3 molecules emitted from the patient's breath (e.g., renal disease and halitosis) (Lee et al. 2020; Li et al. 2018; Cha et al. 2018). Moreover, we confirmed that the effect of relative humidity (20 – 99%) on the response to electric current was negligible (Fig. 5d).

Mechanical flexibility is an essential factor for various practical applications in wearable devices (Lee et al. 2020). For mechanical flexibility, 1,000 bending cycles were performed on RGOLF (Fig. 6). As shown in the schematic, the elongation and compression of RGOLF proceeded as a single bending cycle. The RGOLF exhibited no dramatic changes in the electrical response (1.14% of variation) during the 1,000 cycles of the bending test. This indicates that the RGOLF exhibited outstanding flexibility. Based on the flexibility test, RGOLF could be a candidate for a wearable sensor based on graphene e-textiles for detecting toxic gas molecules in the environment. Also, it can be used to monitor human health (e.g., kidney disease, halitosis, and cancer) by detecting specific gas molecules from the patient's breath (Di Natale et al. 2014; Chan et al. 2020; Kahn et al. 2015).

4. Conclusions

We demonstrated graphene e-textiles (RGOLF) that were fabricated by coating graphene flakes on bioinspired LF. Compared to conventional graphene e-textiles, RGOLF exhibited a higher electrical conductivity (4.63 ± 0.22 μS) with use of the same concentration of graphene. Moreover, the RGOLF is based on cellulose fiber and therefore very light (< 1 mg), which would be a great advantage for wearable applications such as e-textiles. We optimized the GO concentration and diameter of the LF, which showed high electrical conductivity. The higher the GO concentration and LF diameter, the higher was the electrical conductivity of RGOLF. We verified the possibility of RGOLF as a wearable application through NO_2 gas exposure and mechanical flexibility tests. From the practical experiment, we confirmed that the RGOLF has a potential candidate for a wearable gas sensor to detect toxic NO_2 gas from environmental air. The RGOLF showed a good sensing performance to NO_2 with a low detection limit (~1 ppm), high selectivity, and resistance to relative humidity. This means that the RGOLF could be used as a NO_2 gas leakage alarm system in industrial areas or living environments. Furthermore, the mechanical flexibility test exhibited the outstanding flexibility of the RGOLF, supporting its applicability as a wearable gas sensor. Taken together, our results demonstrate that the bioinspired RGOLF has the potential to be used in various wearable applications such as gas sensors for detecting hazardous gas molecules in environmental air, and exhaled breath sensors for monitoring human health based on human breath. Overall, the RGOLF suggests an eco-friendly, cheap, disposable, and easily fabricated graphene e-textile that can be used in various wearable applications.

Declarations

Acknowledgments

This work was supported by a National Research Foundation of Korea (NRF) Grant funded by the Korean Government (MSIP) (No. NRF-2020R1A2C2102262, NRF-2019R1A2B5B01070617, and NRF-2020R1A6A3A01096477). This study was also supported by a Korea University Grant and the BK21 FOUR (Fostering Outstanding Universities for Research).

References

1. Abdelkader AM, Karim N, Vallés C, Afroj S, Novoselov KS, Yeates SG (2017) Ultraflexible and robust graphene supercapacitors printed on textiles for wearable electronics applications. 2D Materials 4(3):035016. doi:10.1088/2053-1583/aa7d71
2. Cha J-H, Kim D-H, Choi S-J, Koo W-T, Kim I-D (2018) Sub-Parts-per-Million Hydrogen Sulfide Colorimetric Sensor: Lead Acetate Anchored Nanofibers toward Halitosis Diagnosis. Anal Chem 90(15):8769–8775. doi:10.1021/acs.analchem.8b01273
3. Chan M-J, Li Y-J, Wu C-C, Lee Y-C, Zan H-W, Meng H-F, Hsieh M-H, Lai C-S, Tian Y-C (2020) Breath Ammonia Is a Useful Biomarker Predicting Kidney Function in Chronic Kidney Disease Patients. Biomedicines 8(11):468
4. Chen Y, Pötschke P, Pionteck J, Voit B, Qi H (2018) Smart cellulose/graphene composites fabricated by in situ chemical reduction of graphene oxide for multiple sensing applications. Journal of Materials Chemistry A 6(17):7777–7785. doi:10.1039/C8TA00618K
5. Chun S, Son W, Kim DW, Lee J, Min H, Jung H, Kwon D, Kim AH, Kim Y-J, Lim SK, Pang C, Choi C (2019) Water-Resistant and Skin-Adhesive Wearable Electronics Using Graphene Fabric Sensor with Octopus-Inspired Microsuckers. ACS Appl Mater Interfaces 11(18):16951–16957. doi:10.1021/acsami.9b04206
6. Coyle S, Wu Y, Lau K-T, Brady S, Wallace G, Diamond D Bio-sensing textiles - Wearable Chemical Biosensors for Health Monitoring. In, Berlin, Heidelberg, 2007. 4th International Workshop on Wearable and Implantable Body Sensor Networks (BSN 2007). Springer Berlin Heidelberg, pp 35-39
7. Di Natale C, Paolesse R, Martinelli E, Capuano R (2014) Solid-state gas sensors for breath analysis: A review. Anal Chim Acta 824:1–17
8. Elsayed NM (1994) Toxicity of nitrogen dioxide: an introduction. Toxicology 89:161–174
9. Ferrari AC, Basko DM (2013) Raman spectroscopy as a versatile tool for studying the properties of graphene. Nat Nanotechnol 8:235. doi:10.1038/nnano.2013.46
10. Hu X, Huang T, Liu Z, Wang G, Chen D, Guo Q, Yang S, Jin Z, Lee J-M, Ding G (2020) Conductive graphene-based E-textile for highly sensitive, breathable, and water-resistant multimodal gesture-distinguishable sensors. Journal of Materials Chemistry A 8(29):14778–14787. doi:10.1039/D0TA04915H
11. Johansson L-S, Campbell JM, Rojas OJ (2020) Cellulose as the in situ reference for organic XPS. Why? Because it works. Surf Interface Anal 52(12):1134–1138. doi:https://doi.org/10.1002/sia.6759
12. Ju Yun Y, Hong WG, Choi N-J, Hoon Kim B, Jun Y, Lee H-K (2015) Ultrasensitive and Highly Selective Graphene-Based Single Yarn for Use in Wearable Gas Sensor. Sci Rep 5:10904. doi:10.1038/srep10904
13. Kahn N, Lavie O, Paz M, Segev Y, Haick H (2015) Dynamic Nanoparticle-Based Flexible Sensors: Diagnosis of Ovarian Carcinoma from Exhaled Breath. Nano Lett 15(10):7023–7028. doi:10.1021/acs.nanolett.5b03052

14. Kan C-W, Lam Y-L (2021) Future Trend in Wearable Electronics in the Textile Industry. Applied Sciences 11(9):3914
15. Kang M-A, Ji S, Kim S, Park C-Y, Myung S, Song W, Lee SS, Lim J, An K-S (2018) Highly sensitive and wearable gas sensors consisting of chemically functionalized graphene oxide assembled on cotton yarn. RSC Advances 8(22):11991–11996. doi:10.1039/C8RA01184B
16. Kinnamon DS, Krishnan S, Brosler S, Sun E, Prasad S (2018) Screen Printed Graphene Oxide Textile Biosensor for Applications in Inexpensive and Wearable Point-of-Exposure Detection of Influenza for At-Risk Populations. Journal of The Electrochemical Society 165(8):B3084–B3090. doi:10.1149/2.0131808jes
17. Lee SW, Jung HG, Jang JW, Park D, Lee D, Kim I, Kim Y, Cheong DY, Hwang KS, Lee G, Yoon DS (2021a) Graphene-based electronic textile sheet for highly sensitive detection of NO_2 and NH_3. Sens Actuators B 345:130361. doi:https://doi.org/10.1016/j.snb.2021.130361
18. Lee SW, Jung HG, Kim I, Lee D, Kim W, Kim SH, Lee J-H, Park J, Lee JH, Lee G, Yoon DS (2020) Highly Conductive and Flexible Dopamine–Graphene Hybrid Electronic Textile Yarn for Sensitive and Selective NO_2 Detection. ACS Appl Mater Interfaces 12(41):46629–46638. doi:10.1021/acsami.0c11435
19. Lee SW, Lee W, Hong Y, Lee G, Yoon DS (2018a) Recent advances in carbon material-based NO_2 gas sensors. Sens Actuators B 255:1788–1804. doi:https://doi.org/10.1016/j.snb.2017.08.203
20. Lee SW, Lee W, Kim I, Lee D, Park D, Kim W, Park J, Lee JH, Lee G, Yoon DS (2021b) Bio-Inspired Electronic Textile Yarn-Based NO_2 Sensor Using Amyloid–Graphene Composite. ACS Sensors 6(3):777–785. doi:10.1021/acssensors.0c01582
21. Lee SW, Lee W, Lee D, Choi Y, Kim W, Park J, Lee JH, Lee G, Yoon DS (2018b) A simple and disposable carbon adhesive tape-based NO_2 gas sensor. Sens Actuators B 266:485–492. doi:https://doi.org/10.1016/j.snb.2018.03.161
22. Leenaerts O, Partoens B, Peeters FM (2008) Adsorption of H_2O, NH_3, CO, NO_2 and NO on graphene: A first-principles study. Phys Rev B 77(12):125416
23. Li H-Y, Lee C-S, Kim DH, Lee J-H (2018) Flexible Room-Temperature NH_3 Sensor for Ultrasensitive, Selective, and Humidity-Independent Gas Detection. ACS Appl Mater Interfaces 10(33):27858–27867
24. Li P, Zhao L, Jiang Z, Yu M, Li Z, Zhou X, Zhao Y (2019) A wearable and sensitive graphene-cotton based pressure sensor for human physiological signals monitoring. Sci Rep 9(1):14457. doi:10.1038/s41598-019-50997-1
25. Liu L, Yu Y, Yan C, Li K, Zheng Z (2015a) Wearable energy-dense and power-dense supercapacitor yarns enabled by scalable graphene–metallic textile composite electrodes. Nat Commun 6(1):7260. doi:10.1038/ncomms8260
26. Liu L, Yu Y, Yan C, Li K, Zheng Z (2015b) Wearable energy-dense and power-dense supercapacitor yarns enabled by scalable graphene–metallic textile composite electrodes. Nat Commun 6:7260. doi:10.1038/ncomms8260

27. Moon IK, Lee J, Ruoff RS, Lee H (2010) Reduced graphene oxide by chemical graphitization. Nat Commun 1:73. doi:10.1038/ncomms1067
28. Ou JZ, Ge W, Carey B, Daeneke T, Rotbart A, Shan W, Wang Y, Fu Z, Chrimes AF, Wlodarski W, Russo SP, Li YX, Kalantar-zadeh K (2015) Physisorption-Based Charge Transfer in Two-Dimensional SnS_2 for Selective and Reversible NO_2 Gas Sensing. ACS Nano 9(10):10313–10323. doi:10.1021/acsnano.5b04343
29. Pandey R, Sinha MK, Dubey A (2020) Cellulosic fibers from Lotus (Nelumbo nucifera) peduncle. J Nat Fibers 17(2):298–309. doi:10.1080/15440478.2018.1492486
30. Park HJ, Kim W-J, Lee H-K, Lee D-S, Shin J-H, Jun Y, Yun YJ (2018) Highly flexible, mechanically stable, and sensitive NO_2 gas sensors based on reduced graphene oxide nanofibrous mesh fabric for flexible electronics. Sens Actuators B 257:846–852. doi:https://doi.org/10.1016/j.snb.2017.11.032
31. Sangita Tomar NY (2019) Lotus Fiber: A Eco Friendly Textile Fiber. International Archive of Applied Sciences Technology 10(2):209–2015
32. Stoppa M, Chiolerio A (2014) Wearable electronics and smart textiles: a critical review. Sensors 14(7):11957–11992. doi:10.3390/s140711957
33. Utari L, Septiani NLW, Suyatman, Nugraha, Nur LO, Wasisto HS, Yuliarto B (2020) Wearable Carbon Monoxide Sensors Based on Hybrid Graphene/ZnO Nanocomposites. IEEE Access 8:49169–49179. doi:10.1109/ACCESS.2020.2976841
34. Wang J, Lu C, Zhang K (2020) Textile-Based Strain Sensor for Human Motion Detection. ENERGY ENVIRONMENTAL MATERIALS 3(1):80–100. doi:https://doi.org/10.1002/eem2.12041
35. Wu M, Shuai H, Cheng Q, Jiang L (2014) Bioinspired Green Composite Lotus Fibers. Angew Chem Int Ed 53(13):3358–3361. doi:https://doi.org/10.1002/anie.201310656
36. Xu M, Huang Q, Wang X, Sun R (2015) Highly tough cellulose/graphene composite hydrogels prepared from ionic liquids. Ind Crops Prod 70:56–63. doi:https://doi.org/10.1016/j.indcrop.2015.03.004
37. Yun YJ, Ah CS, Hong WG, Kim HJ, Shin J-H, Jun Y (2017) Highly conductive and environmentally stable gold/graphene yarns for flexible and wearable electronics. Nanoscale 9(32):11439–11445. doi:10.1039/C7NR04384H
38. Yun YJ, Hong WG, Kim W-J, Jun Y, Kim BH (2013) A Novel Method for Applying Reduced Graphene Oxide Directly to Electronic Textiles from Yarns to Fabrics. Adv Mater 25(40):5701–5705
39. Zhu J, Cho M, Li Y, He T, Ahn J, Park J, Ren T-L, Lee C, Park I (2021) Machine learning-enabled textile-based graphene gas sensing with energy harvesting-assisted IoT application. Nano Energy 86:106035. doi:https://doi.org/10.1016/j.nanoen.2021.106035

Figures

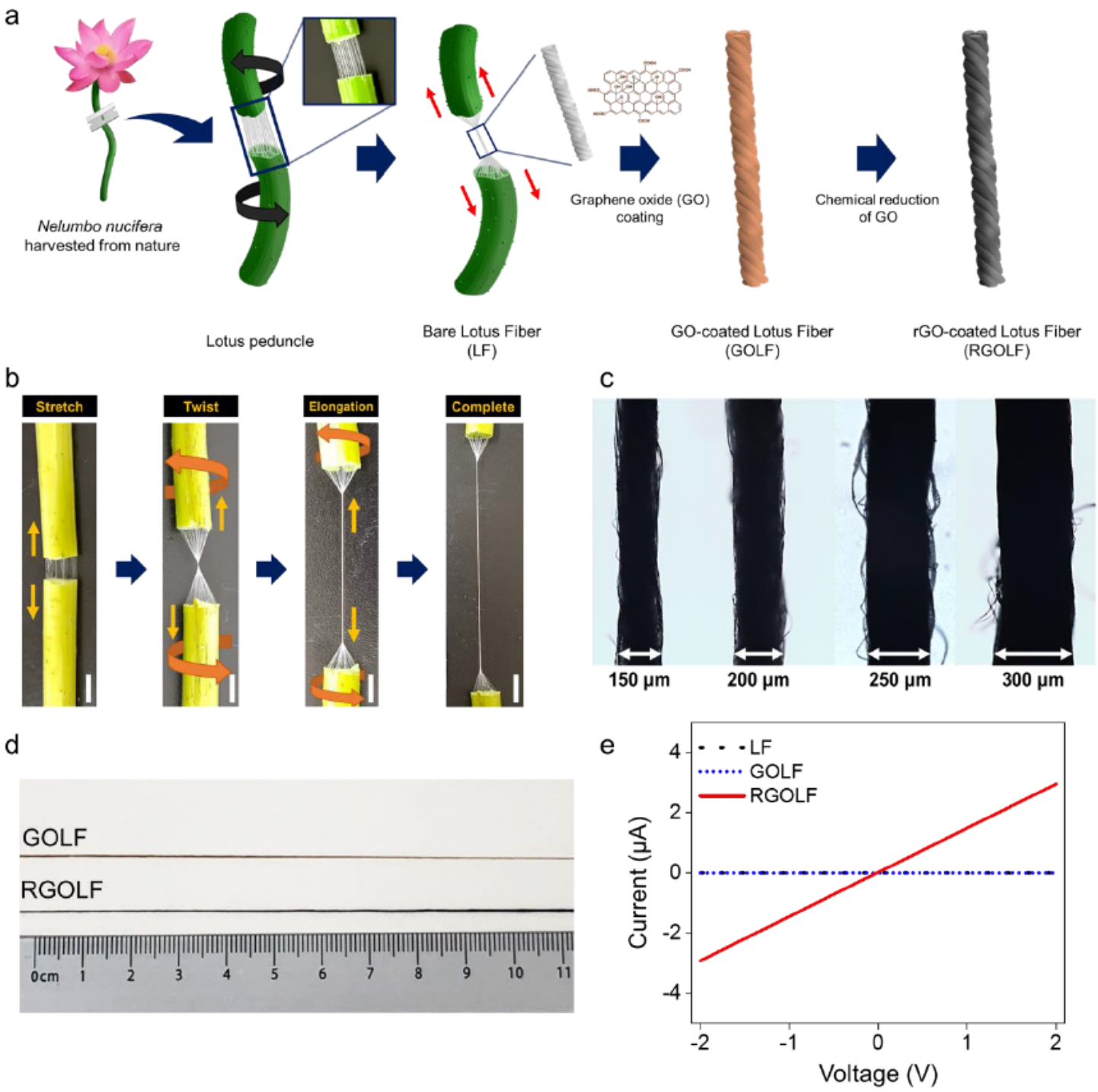

Figure 1

(a) Schematic illustration of a fabrication process for bioinspired graphene-coated lotus fiber (RGOLF). Details are described in the Experimental Section. (b) Photos illustrate the steps for preparing bare lotus fiber (LF) from the stem of Nelumbo nucifera. (The white scale bar: 2 cm) (c) Microscopic image of bare LFs with various diameters (from left to right: 150, 200, 250, and 300 μm). (d) The photo image shows a fabricated GOLF, and RGOLF. (e) Electrical characteristics of the LF, GOLF, and RGOLF were measured by using a current-voltage meter at the applied voltage (from -2 V to 2 V).

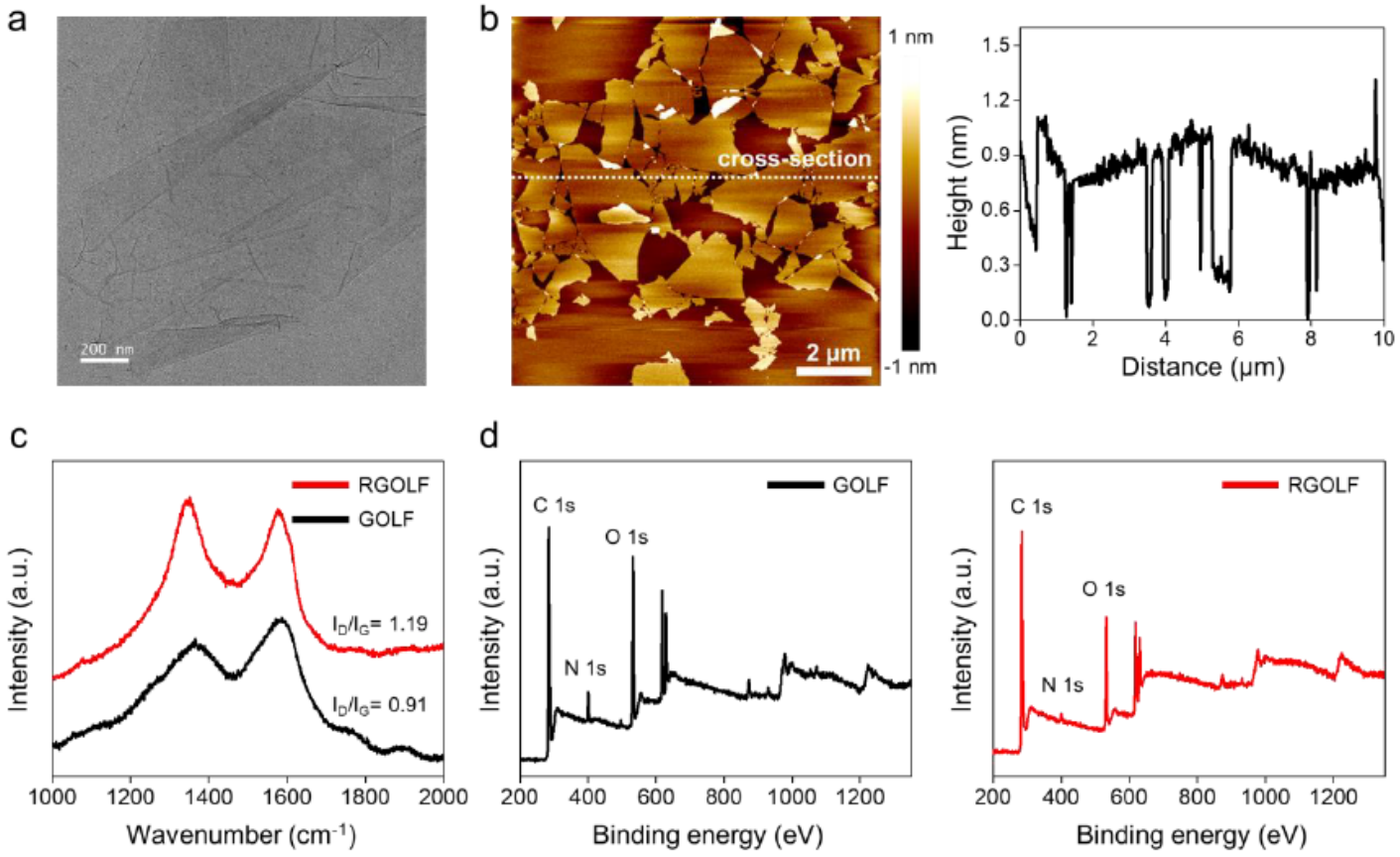

Figure 2

(a) FE-TEM image of GO flakes. (b) High-resolution AFM image and height information of GO flakes. The height of GO flakes was extracted from cross-sectional scan (white dot line) of the AFM image (size: 10 × 10 μm2). (c) Raman spectroscopy and (d) XPS of the fiber before (GOLF) and after (RGOLF) GO reduction.

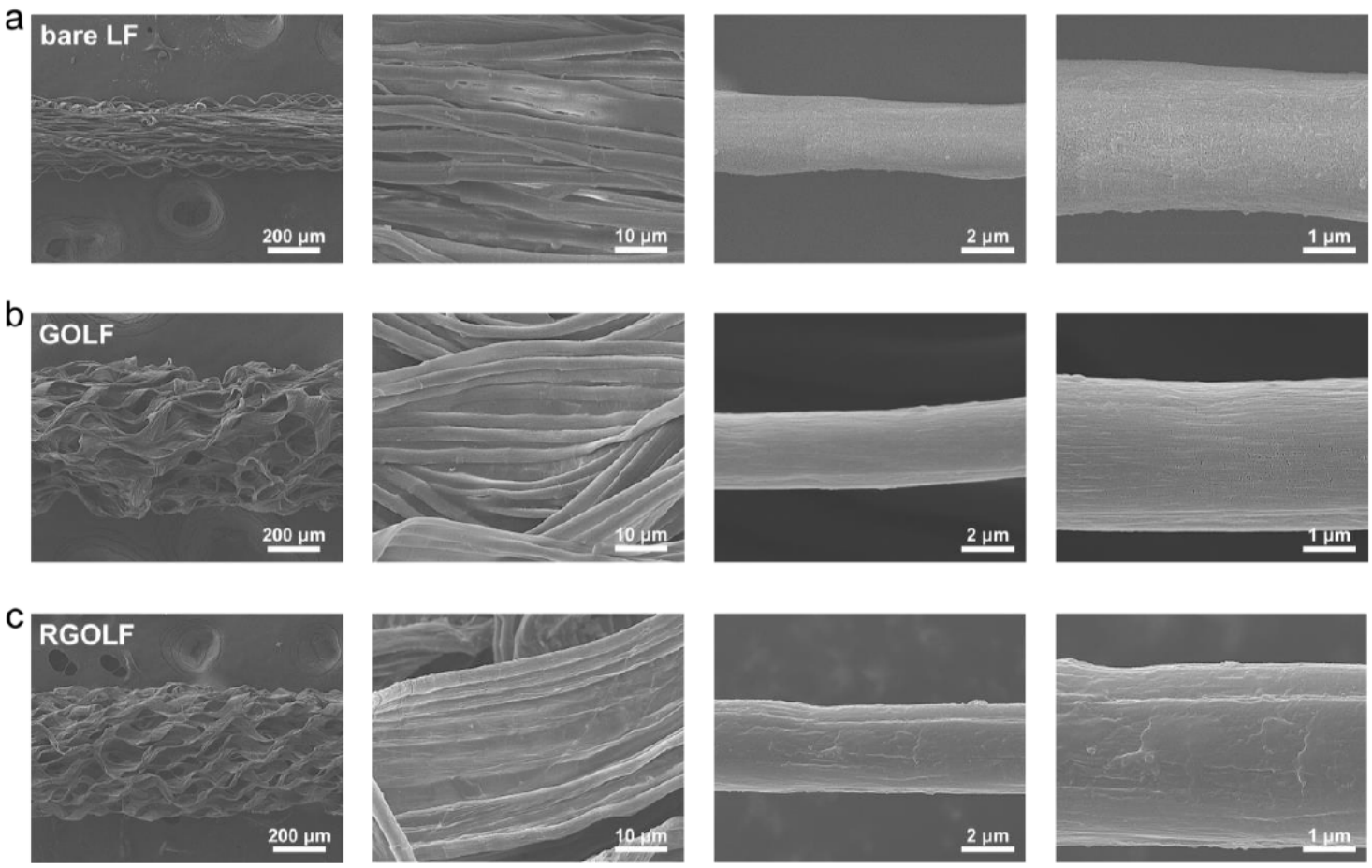

Figure 3

SEM images of (a) the bare LF, (b) the GOLF, and (c) the RGOLF.

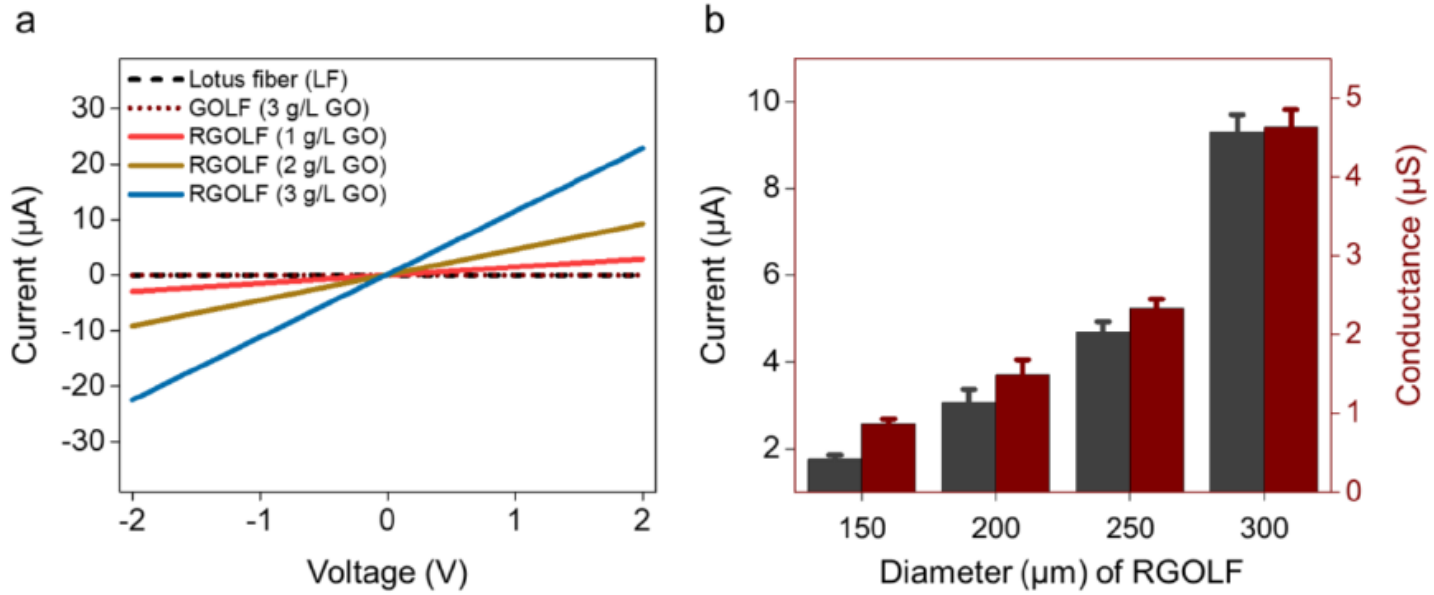

Figure 4

Electrical characterization of the RGOLF via (a) various concentrations (1 – 3 g/L) of GO, and (b) the fiber diameter (150 – 300 μm). Each data point represents triplicate measurements.

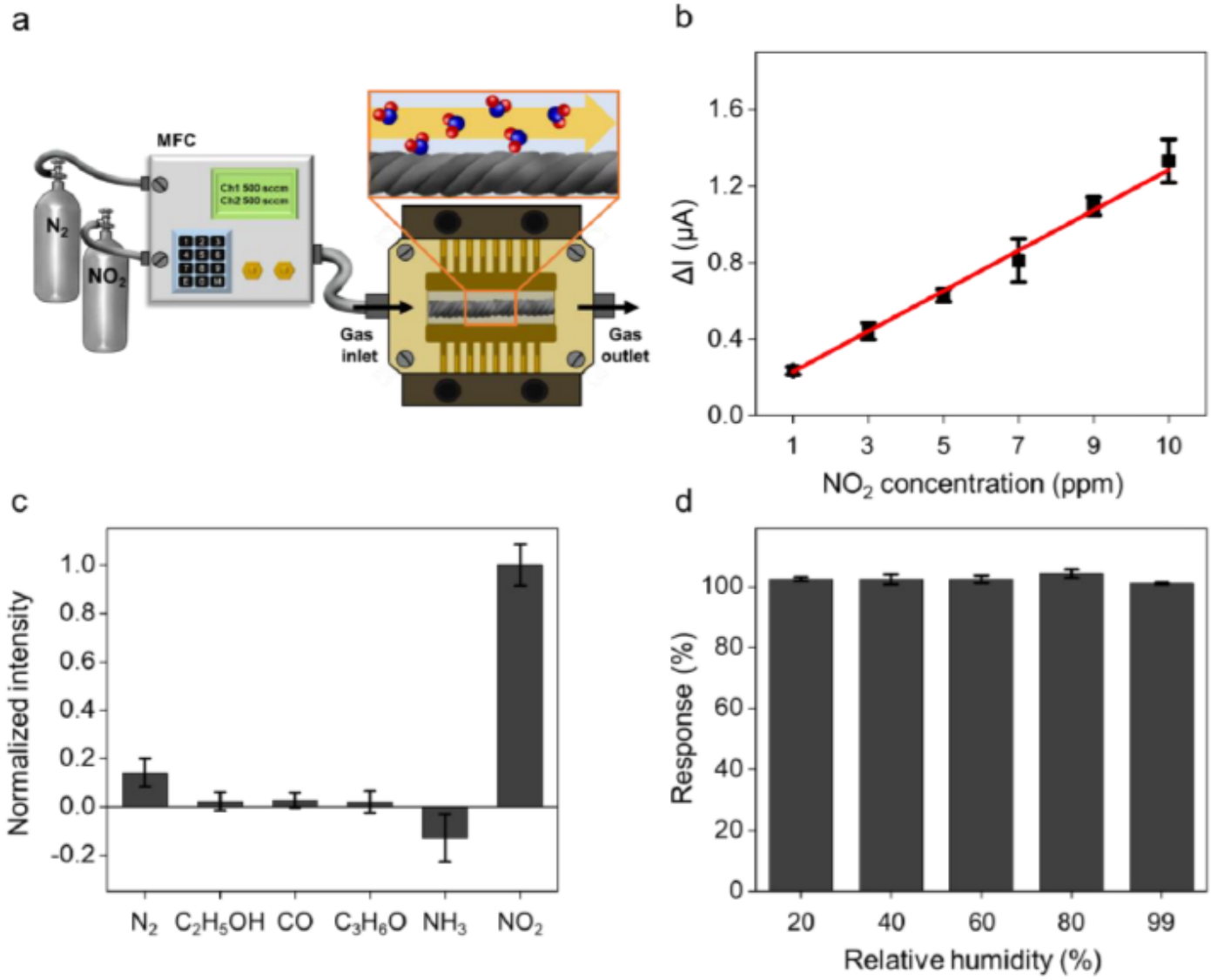

Figure 5

Application of the RGOLF as an electrochemical gas sensor. (a) Schematic of the gas sensing process. (b) Electric current change (ΔI) of the RGOLF with various NO2 concentrations (0 – 10 ppm). (c) Normalized responses of the RGOLF under various gas exposures. The RGOLFs were exposed to various gases including N2 (99%), C2H5OH (100 ppm), CO (10 ppm), C3H6O (100 ppm), NH3 (100 ppm), and NO2 (10 ppm), respectively. (d) Electrical responses of the RGOLF exposed to relative humidity (20 – 99%). Each data point represents triplicate measurements.

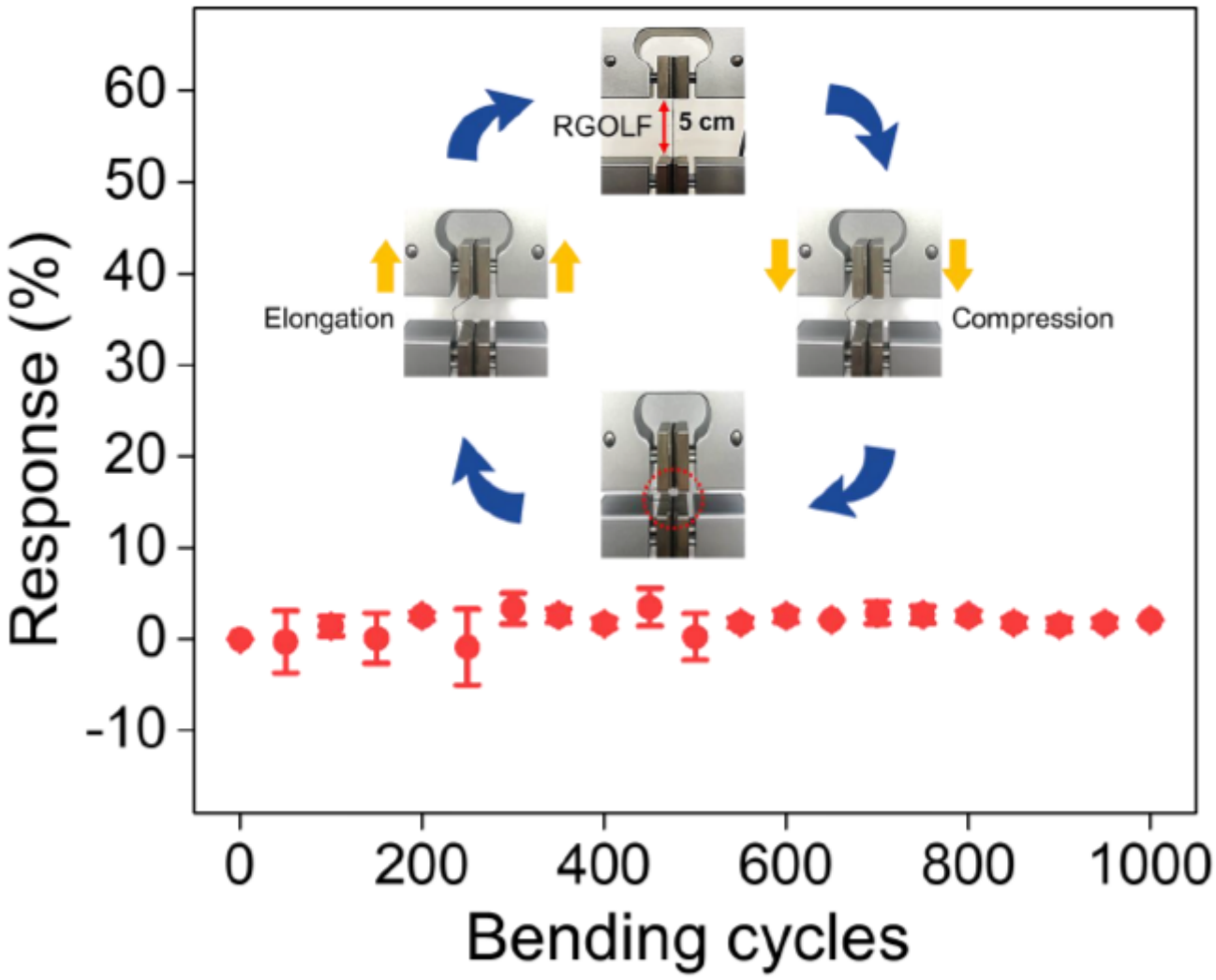

Figure 6

Electrical responses of the RGOLF upon repeated bending cycles (up to 1,000 times). The inserted schematics show one process cycle for the bending test. Each data point represents double measurements.

Supplementary Files

This is a list of supplementary files associated with this preprint. Click to download.

- SupplementaryInformation.docx